Heterojunction LEDs

DOI: 10.1002/smll.200600479

ZnO-Nanowire-Inserted GaN/ZnO Heterojunction Light-Emitting Diodes**

*Min-Chang Jeong, Byeong-Yun Oh, Moon-Ho Ham, Sang-Won Lee, and Jae-Min Myoung**

Nanowires have drawn considerable interest as ideal building blocks for electronics and optoelectronics. Prototype devices based on a single nanowire, such as field-effect transistors (FETs), optical switches, and sensors, verified that nanowires could efficiently transfer carriers.[1–4] In addition, the high injection current and light emission with quantum effect at nanosized junctions, which were formed by crossing p- and n-type nanowires, indicated that high-performance devices could be developed by employing nanowires in their structures.[5,6] ZnO nanowires are one of the most promising materials for short-wavelength semiconductor applications that exploit their simple fabrication processes and superior properties, such as high crystalline quality and lasing effect, in addition to their desirable properties as wide-bandgap semiconductors.[7,8] However, the application of ZnO nanowires to homojunction diodes has been limited due to the absence of reliable p-doping processes and manipulation technologies for junction fabrication, although much progress has been made in these areas. As an alternative approach to utilize ZnO nanowires for optoelectronic applications, a ZnO nanowire/p-GaN film heterojunction structure was suggested, and high efficiency from this junction was expected by improving carrier injection efficiency through the nanosized junctions demonstrating development potential.[9]

Herein, ZnO-nanowire-inserted GaN/ZnO heterojunction light-emitting diodes (LEDs) were obtained by fabricating p^+-GaN film/n-ZnO nanowire array/n^+-ZnO film structures. The self-assembled, nanosized heterojunctions for high injection current were formed by growing n-ZnO nanowire arrays on Mg-doped p^+-GaN films. Moreover, Al-doped n^+-ZnO films were continuously fabricated on the n-ZnO nanowire arrays, for supplying electrons to the heterojunctions through the nanowires and depositing metal contacts on the films without complicated manipulation processes. Blue electroluminescence (EL) emission was observed from the nanowire-inserted heterojunction diodes under forward bias. In addition, the nanowire-inserted GaN/ZnO heterojunction diodes exhibited improved EL emission and electrical characteristics compared to those of the film-based GaN/ZnO heterojunction diodes. As the blue light was emitted by a high injection current through the nanosized heterojunction interface, it is proposed that the development of efficient GaN/ZnO heterojunction LEDs using ZnO nanowires would be possible.

ZnO-nanowire-inserted GaN/ZnO heterojunctions for LED applications were fabricated by growing Mg-doped GaN films, ZnO nanowire arrays, and Al-doped ZnO films in order (see Figure 1a). The Mg-doped GaN films with a thickness of 0.6 μm were epitaxially grown on GaN(0002) templates by molecular beam epitaxy (MBE).[10] ZnO nanowires (32 ± 4.3) nm in diameter and 600 nm in length were subsequently fabricated on the Mg-doped GaN films by metal–organic chemical vapor deposition (MOCVD) to form nanosized GaN/ZnO heterojunctions.[11] The nanosized heterojunctions were expected to have good interfacial contacts because the nanosized contact area and the small lattice mismatch of 1.9% between GaN and ZnO led to epitaxial growth of the ZnO nanowires on the Mg-doped GaN films. The Mg-doped GaN films exhibited p-type conductivity with a hole concentration of 1.2×10^{18} cm^{-3} and hole mobility of 15 $cm^2 V^{-1} s^{-1}$. In addition, the evaluated electron concentration of the n-ZnO nanowires was approximately 10^{12} cm^{-3}.[12] As a result, the Mg-doped GaN film/ZnO nanowire structures made nanosized p^+–n junctions and a wider depletion region in the n-ZnO nanowire side was in-

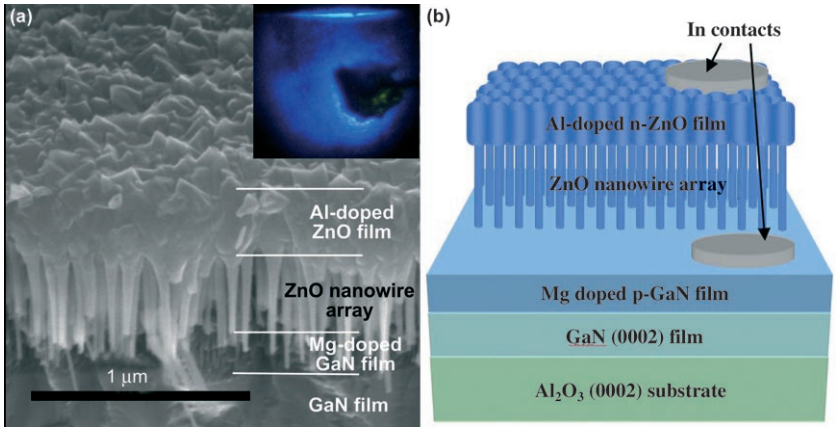

Figure 1. a) A 45°-tilted scanning electron microscopy (SEM) image and b) schematic illustration of the Mg-doped GaN film/ZnO nanowire array/Al-doped ZnO film structures for nanometer-sized GaN/ZnO heterojunction diode applications. The inset is a photograph of blue-light emission from the heterojunction diodes observed through a microscope at the forward current of 10 mA.

[*] M.-C. Jeong, B.-Y. Oh, M.-H. Ham, S.-W. Lee, Prof. J.-M. Myoung
Information and Electronic Materials Research Laboratory
Department of Materials Science and Engineering
Yonsei University,134 Shinchon-Dong, Seoul 120-749 (Korea)
Fax: (+82) 2-365-2680
E-mail: jmmyoung@yonsei.ac.kr

[**] This research was supported by the Second Stage of Brain Korea 21 Project 2006, and the L.G. Philips LCD academic–industrial cooperation program.

duced compared to that of the p^+-GaN film side. To complete the nanowire-inserted heterojunction structures, 0.4-μm-thick Al-doped ZnO films with the high electron concentration of $9.7\times10^{18}\,cm^{-3}$ and an electron mobility of $6.9\,cm^2V^{-1}s^{-1}$ were fabricated on the ZnO nanowire arrays by radio frequency (RF) magnetron sputtering. The Al-doped n^+-ZnO films could supply electrons into the heterojunctions for radiative recombination and the metal electrodes could be fabricated on the n^+-ZnO films without complicated processes. Moreover, the metal contacts on the n^+-ZnO films were more favorable for the formation of ohmic contacts than those directly deposited on the n-ZnO nanowires.

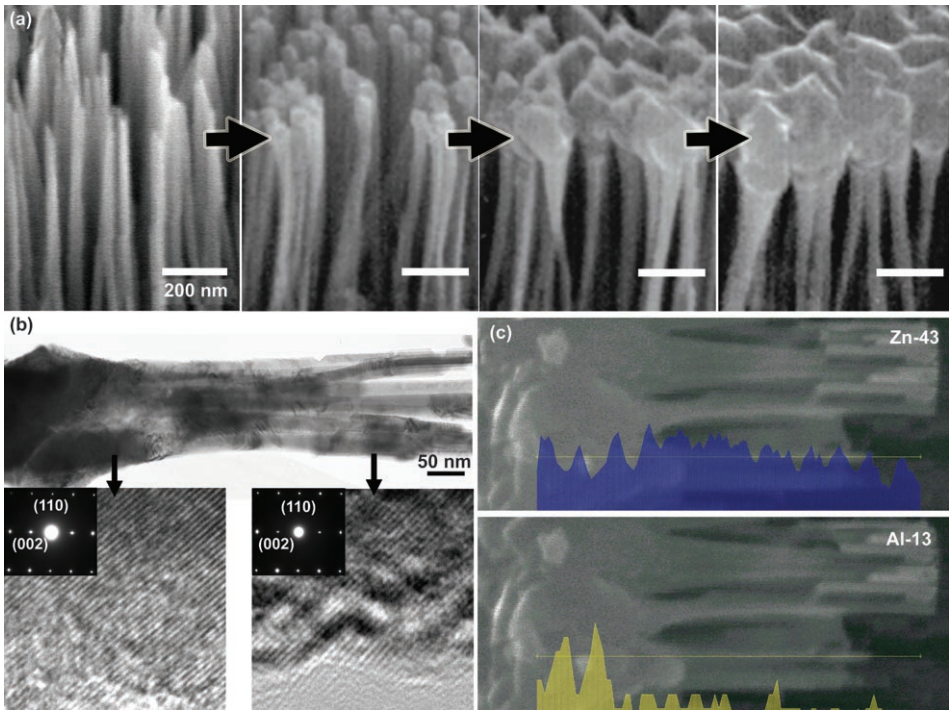

Figure 2. a) SEM images of the tip region of the ZnO nanowires. As-fabricated ZnO nanowires showed a sharp tip-end (left) and the grain size of Al-doped ZnO increased on increasing the deposition time to 0.25, 0.5, and 0.75 h. b) HRTEM image of the Al-doped ZnO film/ZnO nanowire structures and SAED patterns of the film and the nanowire structures. c) EDX profiles of Zn and Al to show the formation region of Al-doped ZnO films fabricated by sputtering.

The final feature of the ZnO-nanowire-inserted GaN/ZnO heterojunction diodes for characterizing the device performance is schematically illustrated in Figure 1b. Film-based ZnO/GaN heterojunction diodes were also fabricated to comparatively investigate the EL emission and carrier injection characteristics of the ZnO-nanowire-inserted GaN/ZnO heterojunction diodes. Al-doped ZnO films with a thickness of 0.5 μm were directly deposited on the MBE-grown, Mg-doped GaN films using RF magnetron sputtering at the optimized temperature of 800 K to minimize the density of interfacial defects and enhance the crystalline characteristics of the films. The electron concentration and mobility of the Al-doped ZnO films were $3.7\times10^{17}\,cm^{-3}$ and $9.4\,cm^2V^{-1}s^{-1}$, respectively.

Interfacial structures between the ZnO nanowires and the Al-doped ZnO films were estimated by observing the morphology changes of the deposited Al-doped ZnO structures on the ZnO nanowires as a function of the deposition time. As shown in Figure 2a, the sputtered materials from an Al-doped ZnO target started to be deposited on the tip of the nanowires and they formed single Al-doped ZnO grains on each nanowire. On increasing the deposition time, the grain size gradually increased and the film structures were eventually fabricated by the grains merging on the nanowires. This observation indicated that the Al-doped ZnO films were continuously fabricated on the nanowires without alternation of crystalline structures at the interface. The high-resolution transmission electron microscopy (HRTEM) images and selected area electron diffraction (SAED) patterns also supported the continuous crystalline structure at the interface between the ZnO nanowires and the Al-doped ZnO films. As shown in Figure 2b, the polycrystalline Al-doped ZnO films and the single-crystalline ZnO nanowires had the same hexagonal structure with crystalline orientation along the *c* axis. The deposition region of the sputtered materials from an Al-doped ZnO target in the heterojunction structures was also defined by performing energy-dispersive X-ray (EDX) analyses using the line-scanning mode along the length direction of the ZnO nanowires (see Figure 2c). A uniform Zn concentration profile was observed in the Al-doped ZnO films and the nanowires. However, Al distribution was identified only in the Al-doped ZnO films, as exhibited in the Al concentration profile, which supports the notion that the Al-doped ZnO films were formed only on the tip of the nanowire arrays. Consequently, the ZnO nanowires and the Al-doped ZnO films formed n–n^+ junctions having good interfacial contacts without crystalline mismatch for electron injection to the p^+–n heterojunction interfaces.

EL emissions from the film-based and the ZnO-nanowire-inserted GaN/ZnO heterojunction diodes were observed under various forward currents. As shown in Figure 3a, the EL spectra of the film-based heterojunction diodes showed broad blue emission peaks. The blue emission peak centered at 440 nm was intensified and blue-shifted to 425 nm on increasing the forward current to 20 mA. Even though the blue emission from the film-based heterojunction diodes was too weak to be detected in the EL spectra at a forward current of 1.5 mA, the blue-light emission was observed by the naked eye. Comparison of Figure 3a

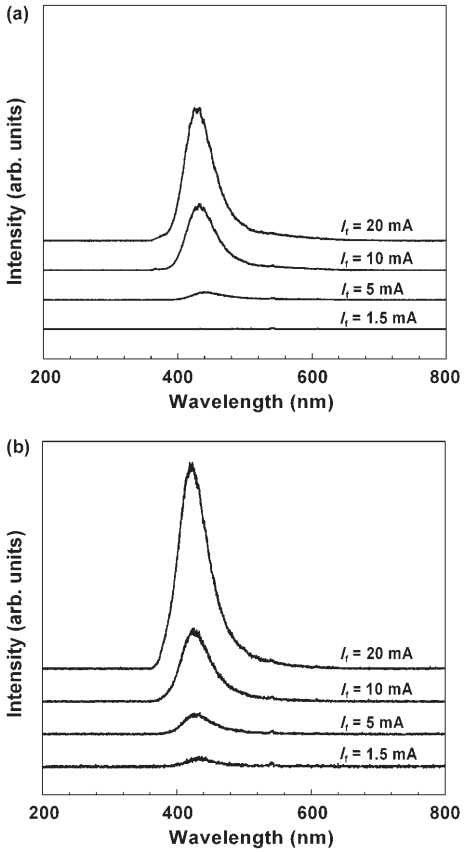

Figure 3. EL spectra of a) film-based GaN/ZnO heterojunction diodes and b) ZnO-nanowire-inserted GaN/ZnO heterojunction diodes.

and b showed that the EL emission from the nanowire-inserted heterojunction diodes was stronger than that of the film-based heterojunction diodes. The nanowire-inserted heterojunction diodes also emitted blue light, at a wavelength of 432 nm even at the low forward current of 1.5 mA. A blue shift to 421 nm and an increased intensity of the EL peak were observed on increasing the forward current to 20 mA. It is expected that the relatively strong intensity and blue shift of the EL peak of the nanosized heterojunction diodes compared to those of the film-based diodes are due to the low density of the interfacial defects, which interrupt the electron injection from ZnO to GaN films.

The origin of the EL emission from the ZnO-nanowire-inserted and film-based GaN/ZnO heterojunction diodes was investigated by comparing the cathodoluminescence (CL) spectra with the EL spectra. The CL spectra were measured by electron-beam irradiation of the Mg-doped GaN films and the Al-doped ZnO films in the nanowire-inserted heterojunction diodes. In addition, the CL spectra of the Al-doped ZnO films directly fabricated on the Mg-doped GaN films were observed (see Figure 4). The CL spectra of the Mg-doped GaN films exhibited a blue emission band centered at 421 nm, which resulted from the band-to-acceptor transition that was generally observed in Mg-doped GaN films due to the deep Mg-related complexes.[10] A UV emission band centered at 389 nm due to the donor-to-band transition was observed in the CL spectra

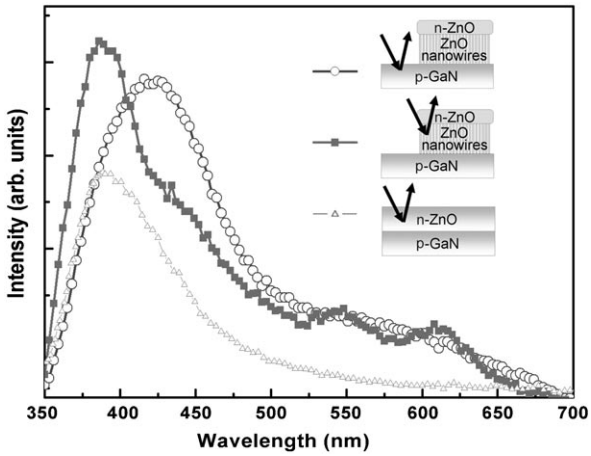

Figure 4. CL spectra of the Mg-doped GaN films, the Al-doped ZnO films fabricated on the nanowire arrays, and the Al-doped ZnO films deposited directly on the Mg-doped GaN films.

of the Al-doped ZnO films.[13] It is assumed that the ZnO nanowires had the same or larger energy bandgap compared to the Al-doped ZnO films, but only the CL emission band from the Al-doped ZnO films was detected in the spectra because the CL emission from the ZnO nanowires was absorbed in the Al-doped ZnO films. The CL spectra of the Al-doped ZnO films in the film-based heterojunction diodes also exhibited the donor-to-band transition centered at 390 nm. These optical properties support the idea that the EL emission from the GaN/ZnO heterojunction diodes was generated from the Mg-doped GaN films.

It was also validated that the blue shift of the EL peak was closely related to the optical properties of the Mg-doped GaN films. At the low injection current from the Al-doped ZnO films and the ZnO nanowires to the Mg-doped GaN films, the blue emission was produced from the conduction band to deep acceptor-level transitions in the Mg-doped GaN films. However, the high injection current enhanced a fast, radiative electron–hole recombination, which increased the strength of the luminescence from the shallow Mg acceptor levels compared to the deep Mg-related levels.[10] Therefore, it is concluded that the EL characteristics of the film-based and nanowire-inserted heterojunction diodes, that is, the intensification and blue shift of the blue emission peaks on increasing the forward current, were due to the electron injection from the ZnO nanowires to the GaN films for radiative electron–hole recombination in the GaN films.

The current–voltage (I–V) characteristics of the film-based and ZnO-nanowire-inserted GaN/ZnO heterojunction diodes were observed (see Figure 5). The I–V curves clearly showed the nonlinear increase of current under the forward bias, and the leakage current of the nanowire-inserted heterojunctions was about 1.5×10^{-6} A, which was three times smaller than that of the film-based heterojunctions at the reverse bias of 10 V. In addition, in the case of the nanowire-inserted heterojunction diodes, the current abruptly increased when the applied voltage exceeded 2.0 V, which was smaller than the turn-on voltage of 2.5 V of the film-based

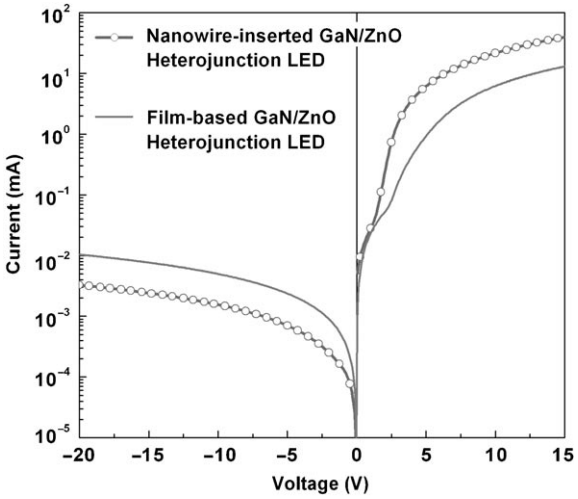

Figure 5. *I–V* curves of the film-based and ZnO-nanowire-inserted GaN/ZnO heterojunction diodes.

heterojunctions, and the abruptly increased current at the applied voltage of 15 V was 2.6 times larger than that of the film-based heterojunction diodes. These different *I–V* characteristics of the nanowire-inserted heterojunction diodes compared to the film-based heterojunction diodes can be explained by energy-band structures at the heterojunction interfaces, that is, the interface between the n-ZnO nanowires and the p^+-GaN films for the nanowire-inserted heterojunctions and the interface between the n-ZnO films and p^+-GaN films for the film-based heterojunctions. The Fermi energy level of the Al-doped ZnO films in the film-based heterojunctions was close to the conduction band compared to that of the ZnO nanowire in the nanowire-inserted heterojunctions, thus resulting in a decrease of the energy barrier at the junction interfaces of the nanowire-inserted heterojunction diodes. In addition, the lattice-matched heterojunction interface, with a low density of interfacial defects and nanosized contacts of the nanowire-inserted heterojunction diodes, reduced the leakage current under the reverse bias and enhanced the electron injection through the heterojunction interface when the forward bias was applied. Therefore, the turn-on voltage of the nanowire-inserted heterojunctions should be small compared to that of the film-based heterojunctions. In addition, the electron–hole recombination was boosted, as a large number of electrons could be injected from the ZnO nanowires to the Mg-doped GaN films without the interruption of interfacial defects.

Capacitance–voltage (*C–V*) characteristics of the film-based and ZnO-nanowire-inserted heterojunction diodes were observed at different frequencies of 10 kHz, 100 kHz, and 1 MHz by applying a reverse bias to evaluate the existence of traps, that is, crystalline defects, at the heterojunction interface (see Figure 6). Defects at the edge of the depletion region affected the capacitance value when the reverse bias was applied to the p–n junctions.[14] As shown in Figure 6a, the capacitance of the film-based heterojunction diodes gradually increased on decreasing the reverse bias, which indicates that the high density of defects was at the

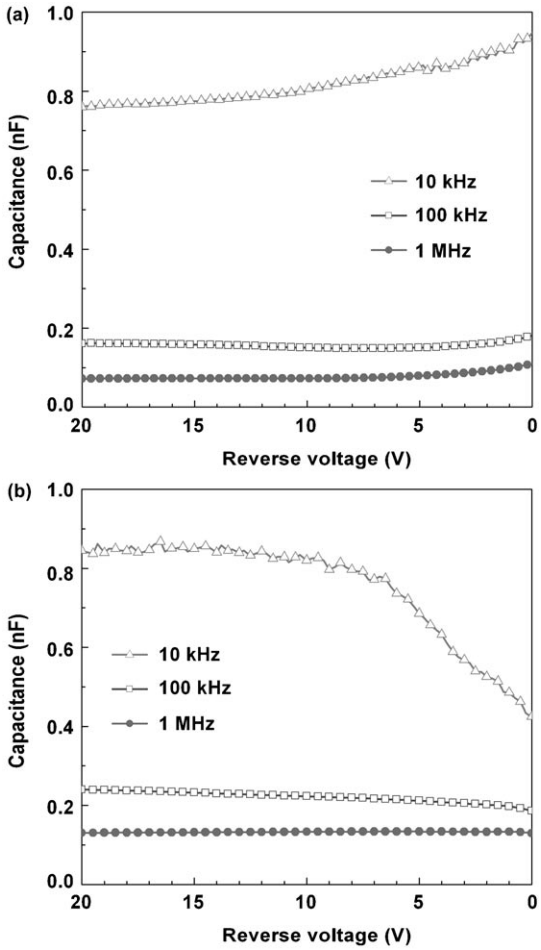

Figure 6. Reverse biased *C–V* curves of a) film-based GaN/ZnO heterojunction diodes and b) ZnO-nanowire-inserted GaN/ZnO heterojunction diodes.

heterojunction interface. In particular, it was expected that the interfacial defects were formed in the ZnO side during film deposition, since the width of the depletion region in the ZnO film side with low electron concentration was wider than that in the GaN film side under the low reverse bias. On the other hand, in the case of the nanowire-inserted heterojunction diodes, even though the capacitance was independent of the reverse bias at the high frequency of 1 MHz, a decrease of the capacitance was observed on decreasing the reverse bias at the low frequencies of 10 and 100 kHz (see Figure 6b). As the capacitance decreased on narrowing the width of the depletion region in the ZnO nanowire side, it was expected that bulk traps, such as the negatively charged oxygen species absorbed on the ZnO nanowires, responded to the low frequencies in the ZnO nanowires. More importantly, the interfacial defects were hardly detected, which was also deduced from almost the same values of capacitance at the reverse bias near 0 V. These results support the proposal that a good heterojunction interface between the p^+-GaN film and the n-ZnO nanowires was formed for carrier injection by inserting the ZnO nanowire arrays in GaN/ZnO heterojunction diodes.

In summary, p^+-GaN film/n-ZnO nanowire array/n^+-ZnO film structures were fabricated to realize efficient heterojunction LEDs using conventional thin-film technologies. The nanowire-inserted heterojunction diodes exhibited improved EL emission and injection current compared to those of film-based heterojunction diodes, due to the nanosized junctions having good interfacial contacts without crystalline defects. It is believed that the nanowire-inserted structures could be applied to other heterojunction systems for device applications and that they will improve the device performance.

Experimental Section

The p^+-GaN films were epitaxially grown on *c*-plane GaN/Al_2O_3 templates by doping with Mg at 923 K in a MBE system. Metallic Ga and Mg were separately introduced to the templates using conventional effusion cells, while nitrogen (6N) was activated and supplied through an inductively coupled RF plasma cell. Details of the growth conditions are given in Ref. [10]. For the fabrication of the ZnO nanowire arrays on the p^+-GaN films, diethylzinc ($(C_2H_5)_2Zn$; Epichem) was supplied to the reactor by Ar carrier gas (6N) as Zn source, and high-purity oxygen (6N) was used as oxidizer in a MOCVD system. The details of the fabrication parameters of the ZnO nanowire array on the GaN templates were the same as those on *c*-plane Al_2O_3 substrates.[11] The 0.4-μm-thick Al-doped ZnO films were fabricated on top of the ZnO nanowire arrays at room temperature and the 0.5-μm-thick Al-doped ZnO films were deposited directly on p^+-GaN films at 800 K by RF magnetron sputtering. The Al-doped ZnO target (3 wt.% Al) was sputtered with RF power 150 W in Ar atmosphere and the working pressure was controlled to 5 mTorr.

The electrical characteristics of the ZnO nanowires were determined by fabricating a back-gate ZnO nanowire FET and measuring its carrier-transfer characteristics. The fabrication and evaluation methods were reported in Refs. [12, 15]. The morphology and structural characteristics of the n^+-ZnO film/n-ZnO nanowire array/p^+-GaN film heterojunction diodes were observed by field-emission SEM (FESEM, Hitachi S4200) with EDX (Kevex SuperDry II) and HRTEM (JEM-4010). EL emissions of the heterojunction diode were observed under forward bias using a scanning monochromator and a sensitive photomultiplier tube (PMT, Hamamatsu). The optical characteristics of the p-GaN films and the n-ZnO nanowire/n^+-ZnO film structures were examined by CL spectroscopy with an acceleration voltage of electron beams of 10 kV. Indium films were formed on ZnO films for ohmic contacts, and the current–voltage (*I–V*) characteristics of the heterojunction diodes were measured using a semiconductor parameter analyzer (HP4145B). In addition, the reverse bias current–voltage (*C–V*) characteristics of the heterojunction diodes were measured at frequencies of 1 kHz, 10 kHz, 100 kHz, and 1 MHz using an LCR meter (Agilent 4284 A).

Keywords:
heterojunctions · interfaces · LEDs · nanowires · zinc oxide

[1] W. I. Park, J. S. Kim, G. C. Yi, H. J. Lee, *Adv. Mater.* **2005**, *17*, 1393.
[2] X. Duan, C. Niu, V. Sahi, J. Chen, J. W. Parce, S. Empedocles, J. L. Goldman, *Nature* **2003**, *425*, 274.
[3] Y. Cui, Q. Wei, H. Park, C. M. Lieber, *Science* **2001**, *293*, 1289.
[4] M. C. Jeong, B. Y. Oh, M. H. Ham, J. M. Myoung, *Appl. Phys. Lett.* **2006**, *88*, 202105.
[5] X. Duan, Y. Huyang, Y. Cui, J. Wang, C. M. Lieber, *Nature* **2001**, *409*, 66.
[6] G. D. J. Smit, S. Rogge, T. M. Klapwijk, *Appl. Phys. Lett.* **2002**, *81*, 3852.
[7] X. Wang, C. J. Summers, Z. L. Wang, *Nano Lett.* **2004**, *4*, 423.
[8] M. H. Huang, S. Mao, H. Feick, H. Yan, Y. Wu, H. Kind, E. Weber, R. Russo, P. Yang, *Science* **2001**, *292*, 1897.
[9] W. I. Park, G. C. Yi, *Adv. Mater.* **2004**, *16*, 87.
[10] J. M. Myoung, K. H. Shim, C. Kim, O. Gluschenkov, K. Kim, S. Kim, D. A. Turnbull, S. G. Bishop, *Appl. Phys. Lett.* **1996**, *69*, 2722.
[11] M. C. Jeong, B. Y. Oh, W. Lee, J. M. Myoung, *J. Cryst. Growth* **2004**, *268*, 149.
[12] T. H. Moon, M. C. Jeong, B. Y. Oh, M. H. Ham, M. H. Jeun, W. Y. Lee, J. M. Myoung, *Nanotechnology* **2006**, *17*, 2116.
[13] Y. Alivov, J. E. Van Nostrand, D. C. Look, M. V. Chukichev, B. M. Ataev, *Appl. Phys. Lett.* **2003**, *83*, 2943.
[14] J. I. Pankove, *Optical Process in Semiconductors*, Dover Publications, New York, **1975**.
[15] M. H. Ham, J. H. Choi, W. Hwang, C. Park, W. Y. Lee, J. M. Myoung, *Nanotechnology* **2006**, *17*, 2203.

Received: September 7, 2006
Revised: November 21, 2006
Published online on February 12, 2007

